miR-34a negatively regulates efferocytosis by tissue macrophages in part via SIRT1

Alexandra L McCubbrey[*], **Joshua D. Nelson**[†], **Valerie R. Stolberg**[§], **Pennelope K. Blakely**[‡], **Lisa McCloskey**[†], **William J. Janssen**[¶,||], **Christine M. Freeman**[†,§], and **Jeffrey L. Curtis**[*,†,#]

[*]Graduate Program in Immunology, University of Michigan Health System, Ann Arbor, MI, 48109

[†]Division of Pulmonary & Critical Care Medicine, Department of Internal Medicine, University of Michigan Health System, Ann Arbor, MI, 48109

[‡]Department of Neurology, University of Michigan Health System, Ann Arbor, MI, 48109

[§]Research Service VA Ann Arbor Healthcare System, Ann Arbor, MI, 48105

[¶]Division of Pulmonary Sciences & Critical Care Medicine, Department of Medicine, University of Colorado Health Sciences Center, Denver

[||]Department of Medicine, National Jewish Health, Denver, CO 80262

[#]Pulmonary & Critical Care Medicine Section, VA Ann Arbor Healthcare System, Ann Arbor, MI, 48105

Abstract

Apoptotic cell (AC) clearance ("efferocytosis") is an evolutionarily conserved process essential for immune health, particularly to maintain self-tolerance. Despite identification of many recognition receptors and intracellular signaling components of efferocytosis, its negative regulation remains incompletely understood, and has not previously been known to involve microRNAs (miRs). Here we show that miR-34a (gene ID 407040), well-recognized as a p53-dependent tumor suppressor, mediates coordinated negative regulation of efferocytosis by resident murine and human tissue macrophages (Mø). miR-34a expression varied greatly between Mø from different tissues, correlating inversely with their capacity for AC uptake. Transient or genetic knockdown of miR-34a increased efferocytosis, whereas miR-34a over-expression decreased efferocytosis, without altering recognition of live, necrotic or Ig-opsonized cells. The inhibitory effect of miR-34a was mediated both by reduced expression of Axl, a receptor tyrosine kinase known to recognize AC, and of the deacetylase SIRT1, which had not previously been linked to efferocytosis by tissue Mø. Exposure to AC down-regulated Mø miR-34a expression, resulting in a positive feedback loop that increased subsequent capacity to engulf AC. These findings demonstrate that miR-34a both specifically regulates and is regulated by efferocytosis. Given the ability of efferocytosis to polarize ingesting Mø uniquely and to reduce their host-defense functions, dynamic negative regulation by miR-34a provides one means of fine-tuning Mø

Address correspondence and reprint requests to: Jeffrey L. Curtis, M.D., Pulmonary and Critical Care Medicine Section (506/111G), Department of Veterans Affairs Healthsystem, 2215 Fuller Road; Ann Arbor, MI 48105-2303, U.S.A., Phone: 734-845-3457 Fax: 734-845-3257, jlcurtis@umich.edu.

behavior towards AC in specific tissue environments with differing potentials for microbial exposure.

Keywords

phagocytosis; microRNA; mice; inbred strains; human

INTRODUCTION

Efferocytosis is the essential, dynamic mechanism by which apoptotic cells (AC) are located, bound, engulfed and degraded. Tight regulation of efferocytosis is necessary to balance beneficial immunogenic responses against pathogens and malignant cells with the fundamental need to prevent autoimmunity. AC engulfment regulates autoimmunity and inflammation both passively by removing self-antigens, and actively by triggering phagocyte secretion of anti-inflammatory mediators including TGF-beta (1–4), IL-10 (5, 6), and PGE$_2$ (7). Hence, controlling both the timing of AC clearance and the cell types mediating efferocytosis assists in resolving inflammation and in initiating tissue repair without excessively impairing host defense.

Virtually any cell type can mediate AC clearance, but mononuclear phagocytes are particularly crucial to understand, due to their greater efferocytic capacity (on a per-cell basis), and the marked immunological consequences of the process on their host defense functions. Mononuclear phagocytes abundantly express receptors that recognize AC cells by directly or indirectly binding phosphatidylserine exposed on the AC outer plasma membrane (8). Among these recognition receptors is the TAM family of receptor tyrosine kinases, which includes Axl (9). Indeed, the differing efferocytic abilities of macrophages (Mø) versus dendritic cells can be explained in part by differences in their patterns of TAM expression (10). AC recognition triggers intracellular signaling through pathways including Protein Kinase C βII, PLC-γ and PI3K (11, 12). Studies in *C. elegans* identified two signaling pathways that culminate in Rac activation via distinct intracellular mediators: one via homologues of mammalian CrkII/ELMO/DOCK180 and another through the homologue of mammalian GULP (13). Both pathways are activated in mammalian cells following AC recognition (14–19). As might be anticipated by the imperative to regulate efferocytosis, the process is controlled both by positive feedback loops (e.g., breakdown products of AC degradation activate 5' adenosine monophosphate-activated protein kinase (AMPK) (20) and Liver X receptor alpha (LXRα) (21), allowing the phagocyte to handle the increased metabolic load), and by several negative regulators of Rac activation (22–28). Dynamically restricting clearance to certain phagocyte subsets is another means of balancing the potentially conflicting consequences of efferocytosis (29).

MicroRNAs (miRs) are short single-stranded RNAs that perform key post-transcriptional regulatory functions (30), in most cases reducing accumulation of proteins translated from the mRNAs that they target. There are over 2500 validated human miRs recorded in miRBase v20 (31), many highly conserved throughout eukaryotes. Each miR may control ~200 genes, so they are believed collectively to regulate up to 60% of all protein-coding

genes (32, 33). The importance of miR-mediated disruption of gene translation in vivo has been shown in numerous pathways including a model of LPS tolerance (34) and myocardial infarction (35). A single example of positive regulation of efferocytosis by miRs has recently been demonstrated in vitro (36), but there are to date no examples of which we are aware of negative regulation of efferocytosis by miRs.

While studying miR regulation of Mø immune responses, we observed a striking inverse correlation in murine resident Mø of different tissues between expression of miR-34a (gene ID 407040) and efferocytic capacity. In this study, we identify miR-34a as a negative regulator of both the surface AC receptor Axl and the intracellular NAD+-dependent deacetylase Silent Information Regulator T1 (SIRT1). Further, miR-34a expression is itself inhibited by efferocytosis, creating a positive feedback loop that enhances subsequent AC uptake and disposal.

MATERIALS AND METHODS

Mice

For all experiments with wild type (wt) mice, C57BL/6 mice were purchased from Jackson Laboratories. Experiments were performed primarily at VA Ann Arbor Healthcare System, with additional experiments at National Jewish Health; both Animal Care Facilities are fully accredited by the American Association for Accreditation of Laboratory Animal Care. Mice were housed under specific pathogen-free conditions and used for experiments between 8–16 weeks of age. To generate miR-34a+/− mice, miR-34a *flox/flox* mice on a C57BL/6 background (37) (Jackson) were crossed with LysM *cre* mice (Jackson). The F1 generation of miR-34a *flox/−* LysM *cre* mice (referred to as miR-34a+/−) was genotyped following Jackson protocols, with non-littermate, age-matched C57BL/6 mice as wt controls in all such experiments. Mice were fed standard animal chow (rodent lab chow 5008; Purina, St. Louis, MO) and chlorinated tap water ad libitum. Animal care and experimentation were conducted in accordance with U.S. Department of Health and Human Services Guide for the Care and Use of Laboratory Animals and were approved by the Animal Use Committee at VA Ann Arbor Healthcare System and National Jewish Health.

Isolation of primary murine Mø cell types

Alveolar cells were collected by bronchoalveolar lavage using 10 ml PBS containing 0.5 mM EDTA (GIBCO, Life Technologies; Grand Island, NY) (25). Cells were plated in lymphocyte culture media (LCM) (10% FBS, 1 mM sodium pyruvate, 0.5 mM 2-Mercaptoethanol, 1 mM HEPES, 100 u/ml penicillin, 100 u/ml streptomycin, 0.292 mg/ml L-Glutamine in RPMI) (all from GIBCO). Alveolar Mø (AMø) were adhesion purified from this population by discarding non-adherent cells after 1.5 h of culture. Unstimulated peritoneal cells were isolated by peritoneal lavage using 10 ml PBS containing 0.5 mM EDTA, administered in 1–2 ml aliquots. Cells were plated in LCM and peritoneal Mø (PMø) were adhesion purified from this population; non-adherent cells were discarded after 45 min of culture. All cultures were performed in a 5% CO_2 environment at 37°C.

To isolate murine bone marrow-derived Mø (BMDMø) (38), bone marrow was collected from murine fibulas and tibias, then disaggregated to a single cell suspension using the same 21 gauge needle and a 70 μm strainer. Bone marrow from one mouse was resuspended in LCM containing 20% FBS; 25 ml of this suspension was plated in a 15 cm non-tissue culture-treated Petri dish, to which GM-CSF (GIBCO) was added at a final concentration of 25 ng/ml. On day 4, 10 ml fresh LCM containing 20% FBS and GM-CSF was added to each plate. On day 7, non-adherent and lightly adherent cells were discarded and adherent cells (BMDMø) were detached by incubating the dishes in cold PBS at 4°C. BMDMø were counted and plated in LCM in tissue culture-treated plates as needed for experiments.

To isolate murine microglia (39, 40), cerebri from mouse pups 2–3 days of age were collected under aseptic conditions and meninges were removed. Cerebri were minced using sharp edged forceps, resuspended in 0.5% trypsin (Biowhittaker, Walkersville, MD, USA), and incubated at 37°C for 20 min. Next, cells were resuspended in DMEM 4.5 g/L glucose, (Biowhittaker) containing 10% fetal bovine serum (Hyclone, Logan, UT, USA), 200 mM L-glutamine, 100 U/ml penicillin, 0.1 mg/ml streptomycin and 0.25 lg/ml fungizone (P/S/F mix, Biowhittaker), OPI medium supplement (oxalacetic acid, pyruvate, insulin, Sigma-Aldrich, St Louis, MO, USA), and 0.5 ng/ml recombinant mouse GM–CSF (BD Pharmingen, San Diego, CA, USA). This cell suspension was filtered through a 70 μm strainer centrifuged at 290 x g for 5 min at 4°C. Cells from a 2–3 mouse brains were resuspended in complete medium containing 5 ng/ml GM-CSF and seeded into 150-cm^2 flasks (Costar, Corning, NY, USA). Cells were maintained in a humidified atmosphere of 95% air/6.5% CO_2. When mixed glial cultures reached confluency (7–10 d), flasks were shaken overnight at 200 rev./min at 37°C to detach microglia from the more firmly adherent astrocytes. Cells in suspension (>95% pure CD11b+ microglia) were collected and plated in LCM in tissue culture-treated plates as needed for experiments.

Human subjects and isolation of resident human AMø

Studies and consent procedures were performed in accordance with the Declaration of Helsinki at the VA Ann Arbor Healthcare System and were approved by its Institutional Review Board (FWA 00000348). All subjects understood the purpose of the study and gave written consent before any research procedures. All subjects underwent a complete history and physical examination by a Pulmonologist, spirometry, chest imaging, prospective collection of medication history, and complete blood count with differential, coagulation studies and chemistry panel. We recruited six healthy volunteers without evidence of lung disease. Clinical characteristics of the human volunteers are shown in Table 1. Subjects underwent bronchoscopy under moderate conscious sedation using a fiberoptic bronchoscope and resident human AMø were isolated by segmental bronchoalveolar lavage, both as recently described in detail (41). Not all subjects were used in every experiment.

Transient transfection of primary macrophages

In some experiments, murine or human AMø and murine PMø, microglia and BMDMø were transiently transfected using Lipofectamine RNAiMAX (Invitrogen, Life Technologies; Grand Island, NY) based on manufacturer's instructions. RNAiMAX and antagomirs [miR-34a-5p antagomir and negative control A (Exiqon; Vedbaek, Denmark)] or mimics

[miR-34a-5p mimic or mimic negative control #1 (Invitrogen)] were diluted separately in OptiMEM (Invitrogen). Diluted RNAiMAX and diluted antagomir or mimic were then combined at 1:1 with a final concentration of 1 μl lipofectamine and 5 pM antagomir/mimic in 50 μl. The RNAiMAX/construct complex was incubated at room temperature for 15 min, then added to cells (50 μL/well in chamber slides or 100 μL/well in 24-well plates). Next, 3x LCM was added to each well to a final volume of 200 μl/well in chamber slides or 400 μl/well in 24-well plates. Cells were incubated 24–48 h to complete transfection.

Chamber slide adhesion and phagocytosis assays

To induce apoptosis, we treated single-cell suspensions of murine thymocytes with 10 mM dexamethasone (Sigma-Aldrich; St. Louis, MO) for 4.5 h. These conditions consistently produced 50–60% Annexin+, propidium iodide- thymocytes, as we have previously shown (11). Necrotic cells were produced by incubating thymocytes at 56°C for 45 min. SRBC (Colorado Serum Company, Denver, CO) were opsonized with anti-SRBC (Sigma) for 1 h, as previously described (11).

Mø were plated at $1–2 \times 10^5$ cells/well in 8-well Permavox chamber slides (Nunc, Thermo Fisher Scientific, Grand Island, NY). Target AC, live cells, necrotic cells or opsonized SRBC were added to Mø at a ratio of 10 targets per phagocyte in LCM containing heat-inactivated serum (HyClone) at a final concentration of 10% as a source of essential opsonins including Gas6 (42), and co-incubated for 0.5–1.5 h incubation in a 5% CO_2 environment at 37°C. Next, slides were collected by removing gaskets and washing in ice-cold PBS containing 0.5 mM EDTA to remove unengulfed targets. Slides were dried, then stained with H&E. To quantify ingested particles of all types, at least 200 Mø were counted at 1000x magnification under oil. The phagocytic index was calculated by dividing the total number of ingested target cells by the total number of Mø counted.

In some experiments, we modified the action of SIRT1 using pharmacological agents at established effective and non-toxic concentrations. For this purpose, we used the agonist resveratrol (Sigma-Aldrich) (43, 44) or the antagonists sirtinol (IC_{50} = 131 nM) (Cayman Chemicals, Ann Arbor, MI) (45, 46) and 6-Chloro-2,3,4,9-tetrahydro-1H-Carbazole-1-carboxamide (EX-527) (IC_{50} = 38 nM) (Sigma-Aldrich) (47, 48). These reagents were initially solublized in DMSO, then diluted in LCM.

TAMRA and pHrodo phagocytosis assays

We also used two flow-cytometric assays of phagocytosis. First, 50×10^6 AC were labeled with 75μg TAMRA (Invitrogen) in 1 ml PBS and 1 ml LCM for 15 min at 37°C (49–51). Labeled AC were washed two times with PBS to remove excess TAMRA. Second, *S. aureus* pre-labeled with pHrodo-green (Invitrogen) was opsonized by incubation in rabbit anti-staphylococcal mAb (Invitrogen) for 1 h in a 5% CO_2 environment at 37°C, then washed . Mø were plated at 3×10^6 cells/well in 24-well plates. Mø pretreated with cytochalasin D (Sigma) for 1 h before exposure to florescent targets were used to establish baseline florescence. TAMRA-labeled AC or pHrodo-green labeled *S. aureus* targets were added to Mø for 1 h, then wells were washed briskly with cold PBS to remove unengulfed targets. Mø were detached from culture dishes using the dissociation enzyme TrypLE (Invitrogen),

then centrifuged in flow tubes. Internalized fluorescent particles were detected by flow cytometry.

Antibodies and Flow Cytometry

Cells were released from culture plates using TrypLE and were stained after Fc-block (Invitrogen) with a panel of directly fluorochrome-conjugated mAbs against the following murine molecules (clone; source): Axl (R&D; Minneapolis, MN); CD4 (L3T4; eBioscience; San Diego, CA); CD8 (CD8b.2; Biolegend; San Diego, CA); CD11b (M1/70; eBioscience); CD11c (N418; eBioscience); CD19 (MCA1439F; AB Serotec); CD44 (IM7; eBioscience); CD45 (30-F11; BD); CD80 (16-10A1; BioLegend); CD206 (C068C2; BioLegend); Ly6C (AL-21; BD); Ly6G (1A8; BD, Franklin Lakes, NJ); Mertk (R&D). Experiments were performed on an LSR II flow cytometer and data were analyzed as previously described (25).

RNA Isolation and RT-PCR

We isolated total RNA from murine AMø, PMø, BMDM and microglia using the RiboPure Kit (Ambion; Grand Island, NY) and removed DNA contamination using the TURBO DNA-free kit (Ambion). cDNA was prepared from total RNA using the RETROscript kit (Ambion). For microRNA amplification, specific cDNA was prepared from total RNA using the TaqMan MicroRNA Reverse Transcription kit. All reagents and kits were used according to the manufacturer's instructions. We performed RT-PCR using TaqMan Gene Expression Master Mix with TaqMan primer-probe sets from Applied Biosystems (Carlsbad, CA) for RNU6B (001093), sno142 (001231), miR-34a (000426), GAPDH (4352932E), SIRT1 (Mm00490758_m1).

Statistical analyses

We calculated significance by one-way ANOVA with Bonferroni or Tukey post hoc testing, Mann-Whitney U test or Student t test, as appropriate, using Prism 6.0g (GraphPad; La Jolla, CA) on an Intel iMac computer. Results were considered significant at $p < 0.05$.

RESULTS

miR-34a negatively regulates efferocytosis by resident murine Mø subtypes

Comparison of miR-34a expression by a variety of resident murine tissue Mø (assayed by quantitative real time PCR) with their capacity to ingest AC in vitro showed a distinct inverse correlation. As we have previously shown in several studies, AMø displayed markedly reduced AC uptake relative to PMø, which was the opposite of their respective miR-34a expression (Fig. 1A) Murine glia and BMDMø displayed intermediate AC uptake that also correlated inversely with their relative expression of miR-34a (Fig. 1A).

To test whether this relationship was causal, we transfected these four murine Mø types to knock down or over-express miR-34a. Transfection of miR-34a-specific antagomirs using the RNAiMAX lipofectamine system significantly decreased miR-34a expression (Supplemental Fig. 1A). In separate experiments using a fluorescently-labeled antagomir, we demonstrated that >90% of cells were transfected using this protocol (Supplemental Fig.

1B) and that transfection did not increase Mø apoptosis (Supplemental Fig. 1C). Knockdown of miR-34a using a specific antagomir significantly increased efferocytosis by murine AMø, glia and BMDMø (Fig. 1B). Conversely, over-expression of miR-34a using a specific mimic significantly decreased the high basal efferocytosis by PMø (Fig. 1B). The results of these microscopy-based assays on murine PMø were corroborated in separate experiments using flow cytometry to assay uptake of TAMRA-stained AC (Supplemental Fig. 2).

To further confirm the ability of miR-34a to down-regulate efferocytosis, we crossed miR-34a *flox*/*flox* and LysM *cre* mice, generating offspring haplosufficient for miR-34a selectively in the myeloid lineage (miR-34a+/−). Haplosufficient heterozygote mice were chosen specifically to investigate the subtle rather than absolute changes induced by modulation of this miR, which we anticipated would more readily mimic its regulation in vivo. Real-time quantitative PCR demonstrated a significant decrease in miR-34a expression in AMø (Supplemental Fig. 3A). These mice developed normally, with no grossly evident abnormalities normal distribution of both lymphoid and myeloid cells in spleen (Supplemental Fig. 3B) and bone marrow (not shown) and normal architecture in spleen, thymus, brain and liver (Supplemental Figs. 3C–F). Resident AMø and BMDMø from miR-34a+/− mice showed increased in vitro efferocytosis compared to AMø and BMDMø from wt mice, respectively (Figs. 1C, 1D). By contrast, AC uptake by resident PMø did not differ between miR-34a +/− mice and wt mice (Figs. 1C, 1D). Together with the results of experiments in which we manipulated miR-34a expression in primary Mø types, these results provide strong evidence that miR-34a is a negative regulator of basal AC engulfment.

miR-34a negatively regulates efferocytosis by resident human AMø

Increased apoptosis of lung parenchymal cells and reduced intra-alveolar efferocytosis have been linked to a variety of chronic lung diseases (52). As in mice, efferocytosis by human AMø is lower than by Mø from other organs, and is even more reduced by smoking (53, 54). Transfection of primary human AMø using the same transfection reagents as in our murine experiments resulted in >98% reduction in miR-34A expression (Fig. 2A); this result is not surprising, as the sequences of the mature miR are identical in the two species. Just as we had seen in mice, knockdown of miR-34a significantly increased efferocytosis by AMø from healthy human never-smokers (Fig. 2B).

miR-34a does not regulate engulfment of live, necrotic, or opsonized cells

To further understand the mechanism by which miR-34a regulates efferocytosis, we tested whether it impacted adhesion of AC. Following knockdown of miR-34a, binding of AC by murine AMø increased, albeit slightly (Fig. 3A). Over-expression of miR-34a using a specific mimic was associated with significantly decreased AC binding by murine PMø (Fig. 3A). Thus, one means by which miR-34a negatively regulates efferocytosis is be reducing initial AC binding, a necessary step preceding engulfment.

To clarify the specificity of miR-34a regulate of Mø behavior, we assessed the effect of manipulating its expression on uptake of non-apoptotic targets. Knockdown of miR-34a in murine AMø did not alter uptake of live or necrotic thymocytes, nor did it alter uptake of Ig-

opsonized SRBC (Fig. 3B). Similarly, over-expression of miR-34a in murine PMø did not alter uptake of Ig-opsonized *Staphylococcus aureus* (Figs. 3C, 3D). Thus, the effect of miR-34a on ingestion by resident murine tissue Mø appears to be specific to efferocytosis.

miR-34a inhibits Axl expression, but does not require Axl to regulate efferocytosis negatively

To identify additional mechanisms by which miR-34a might regulate efferocytosis, we next examined changes in surface expression of multiple AC recognition receptors. Expression of Axl was significantly increased following miR-34a knockdown in AMø, almost doubling MFI (Figs. 4A, 4B). Axl is a known direct target of miR-34a (55) and a key AC recognition receptor (56). In some experimentts, there were small increases in expression of the AC recognition receptors Mertk and CD44 and the Mø activation marker CD80, which did not attain statistical significance, while expression of the mannose receptor CD206 was always unchanged by miR-34a knockdown (not shown). Surface expression of Axl on untreated miR-34a+/− BMDMø was also significantly increased, relative to wt BMDMø (Figs. 4C, 4D).

To test whether upregulation of Axl was obligatory for increased efferocytosis following miR-34a knockdown, we measured efferocytosis in BMDMø from Axl−/− mice (generously provided by the Lemke lab). Knockdown of miR-34a using a specific antagomir increased efferocytosis by Axl−/− BMDMø (Fig. 4E), although the fold-change was small, relative to that seen in BMDMø from wt mice (compare to Figure 1B). Interestingly, basal expression of miR-34a was itself decreased in BMDMø from Axl −/− mice, relative to those of wt mice (Fig. 4F), suggesting possible bidirectional regulation of these gene products. Collectively, these results imply that although Axl is one target through which miR-34a can regulate efferocytosis, Axl-independent pathways of miR-34a action must also exist.

miR-34a inhibits SIRT1, a novel molecule within the AC engulfment pathway

Accordingly, we next tested whether such Axl-independent regulation of efferocytosis by miR-34a could involve the deacetylase SIRT1, another known direct target (57). Indeed, the action of miR-34a as a tumor-suppressor has been attributed in part to negative regulation of SIRT1 (57). Moreover, gene-targeted mice lacking SIRT1 have increased numbers of uncleared AC and develop a lupus-like autoimmunity, potential indicators of defective efferocytosis (58, 59).

We confirmed that basal SIRT1 expression was significantly increased in resident AMø of miR-34a+/− mice, relative to wt mice (Fig. 5A), consistent with the known targeting of SIRT1 by miR-34a. Treating AMø from wt mice with the SIRT1 agonist resveratrol significantly increased their uptake of AC (Fig. 5B). Conversely, treating PMø with the SIRT1 antagonists EX-527 (Fig. 5C) or sirtinol inhibited efferocytosis (Figs. 5D, 5E; Supplemental Fig. 4). By contrast, sirtinol treatment did not affect Fc-mediated uptake by wt PMø of Ig-opsonized SRBC (Figs. 5F, 5G). These data provide support that SIRT1 is another target through which miR-34a negatively regulates efferocytosis.

miR-34a expression is itself inhibited by efferocytosis

Interestingly, initial exposure of murine AMø to AC led to greater efferocytosis during a second exposure to AC 24 h later (Fig. 6A). This finding, an example of enhanced secondary engulfment previously described in other Mø cell types (21), suggested a regulatory mechanism acting by reducing the high basal miR-34a expression in AMø. To explore this possibility, we exposed AMø to AC and measured changes in miR-34a expression by quantitative real-time RT-PCR. After 24 h AC exposure, miR-34a expression was significantly decreased in AMø (Fig. 6B). By contrast, enhanced secondary engulfment was not seen in resident murine PMø (Fig 6C). We did not deem it feasible to determine whether initial AC uptake induced statistically significant further down-regulation in the already very low miR-34A expression by murine PMø. Hence, efferocytosis-induced down-regulation of miR-34a creates a positive-feedback loop to enhance secondary AC engulfment by resident murine AMø.

DISCUSSION

This study shows for the first time that a microRNA, miR-34a, coordinately down-regulates in vitro efferocytosis by resident tissue Mø. Expression of miR-34a varied between resident murine Mø from different tissues, correlating inversely with their AC uptake. Manipulating miR-34a expression, either by transfection or by myeloid-targeted genetic haploinsufficiency, induced reciprocal changes in efferocytosis. This regulatory effect appeared to be specific, as altering miR-34a expression had no effect on uptake of live, necrotic or Ig-opsonized mammalian cells or of an Ig-opsonized bacteria. Knockdown of miR-34a also significantly increased AC uptake by primary human AMø in vitro. We identified a known target of miR-34a, SIRT1, as a novel component of the engulfment machinery of resident tissue Mø. Finally, we showed that miR-34a is itself decreased by AC exposure, permitting enhanced secondary AC uptake. Thus, miR-34a negatively regulates basal efferocytosis by resident Mø in different tissues, but also dynamically permits their efferocytic capacity to rise when AC presence is more prolonged.

Mø and related mononuclear phagocytes such as microglia comprise a sizeable proportion of total cells in all tissues. Efferocytosis strongly reduces Mø ability to respond to microbes (60), to which individual organs are differentially exposed. Accordingly, the avidity of AC uptake by resident Mø must be regulated uniquely in each tissue. This challenge is particularly acute in the gas-exchanging regions of the lungs, where the constant risk of exposure to respiratory pathogens requires prompt responses by the resident AMø. Although it was recently shown that lung epithelial cells clear lung AC in murine models (61), defining how AC so profoundly alters AMø responses to infection remains important.

One strength of the current study is that to increase translational relevance, it was chiefly performed using primary tissue Mø. However, we acknowledge that the experiments using murine BMDMø and microglia involved a period of culture in GM-CSF, which might have influenced the efferocytic capacity of the cells ultimately used experimentally.

miR-34a in the regulation of efferocytosis

Efferocytosis is a highly complex process that exhibits considerable functional redundancy, especially at the level of opsonins and their recognition by surface receptors. It is unlikely that any single factor controls all aspects of AC uptake. However, by coordinately regulating expression of Axl and of the intracellular deacetylase SIRT1, which we discuss below, miR-34a provides one efficient means for tissue-specific regulation of efferocytosis. Given the large number of established miR-34a target genes, it is very likely that miR-34a down-regulates efferocytosis by additional mechanisms. Although verifying this possibility is beyond the scope of the current study, we are particularly interested in known direct targets Notch1 and Notch2, which modulate the functions of Mø and microglia (62, 63), Notch-ligand family members Jagged-1 and Delta-like ligand 1(64, 65), and Wnt1.

That manipulation of miR-34a only modestly changed expression of those molecules was anticipated, because miRs do not typically induce large changes in protein expression of their targeted genes. As stated by Baltimore and colleagues "Because miRNAs appear to provide quantitative regulation of genes, rather than on-off decisions, they can be seen as fine-tuning a cell's responses to external influences" (30). Indeed, a global analysis of the effect of miR-34a over-expression in colon cancer cells found <1.23-fold changes in most targets (66). By contrast, previously identified negative regulators of efferocytosis, including PTEN, CD300a and SIRPα in mammals (24–26, 28) and MTM-1, SRGP-1, SLI-1 and ABL-1 in *C. elegans* (22, 23, 27, 67) all appear to control single molecules that block Rac-driven cytoskeletal changes necessary for AC engulfment. The ability of individual miRs to regulate multiple genes, and the simplicity with which their levels can respond to environmental cues, make miRs ideally suited to regulate complex cellular behaviors dynamically.

Because defective efferocytosis has been associated with a variety of chronic inflammatory lung diseases (52), modulating AC clearance has received considerable attention as a potential broadly applicable therapeutic approach. Indeed, improved efferocytosis might be one mechanism underlying the beneficial effects of statins, macrolides, or corticosteroids in these conditions (25, 68, 69). Nevertheless, it is worth noting that although the high basals levels of miR-34a expression in both murine and human AMø could be reduced to those of murine PMø by transfection of specific antagomirs within 24–48 h, the increase in phagocytic index following treatment of AMø was relatively modest, and did not approach that of PMø, which very avidly ingest AC. Multiple factors determine the reduced basal efferocytic capacity of AMø, including relative reductions in AC adhesion (70) and intracellular signaling pathways (71, 72), and tonic inhibition by lung collectins (24). The degree to which AMø efferocytic capacity can be upregulated remains to be determined, although it is possible that simply increasing it from the depressed state seen in multiple inflammatory lung diseases might still be therapeutically sufficient.

The current findings extend the activities of miR-34a, well-known for its key role as a p53-dependent tumor suppressor that blocks cell division in normal and malignant cells and induces apoptosis in response to genotoxic stress (73). miR-34a resides on human chromosome 1p36.22, a region encoding multiple oncogenes. Reduced miR-34a expression,

either from chromosomal deletion or aberrant methylation of its promoter, is found in a wide range of human malignancies, especially in advanced stages (74). miR-34a also antagonizes metastasis, chemo-resistance and preservation of cancer stem cells. Therapies against specific human cancers based on miR-34a augmentation are in ongoing clinical trials (75). Support for this approach comes from strong anti-tumor effects seen in some transfection studies (76–78). However, anti-tumor immunity depends crucially on dendritic cell cross-presentation of antigens derived from apoptotic tumor cells (79). Our data imply that miR-34a augmentation might inadvertently reduce host anti-tumor responses if it inhibits clearance of apoptotic tumor cells by tumor-associated myeloid cells.

SIRT1 in the regulation of efferocytosis

By showing that inhibitors and agonists of SIRT1 alter AC uptake by resident murine Mø, we also extend the known functions of this molecule. SIRT1 is the founding member of the sirtuin gene family, the mammalian homologues of yeast Sir2 protein. Sirtuins regulate highly diverse cellular processes, including energy balance, stress response, cell/tissue survival and malignancy. At the time we performed these experiments, SIRT1 had not been linked to efferocytosis, although a recent study using the RAW264.7 murine Mø cell line has since provided support for that possibility (80). However, its investigation of a transformed cell line, and use of exposure to oxidized low density lipoprotein both to induce apoptosis and to modulate efferocytosis, make it difficult to compare directly with our study of primary tissue Mø.

Exactly how SIRT1 regulates efferocytosis will require further investigation. SIRT1 is a primarily nuclear-localized class III histone deacetylase (81) that contributes to chromosome remodeling. Importantly, however, SIRT1 also deacetylates multiple non-histone targets, including transcription factors such as forkhead box class O (FoxO) family members, NF-κB, and p53 (82). Because protein levels of p53 depend on acetylation at lysine residue K382, deacetylation by SIRT1 leads to its proteosomal degradation. miR-34a is the gene product most-greatly increased by p53 (66). Hence, by repressing SIRT1, miR-34a creates a positive feedback loop that enhances its own production (74). Additional targets of SIRT1 deacetylation include peroxisome proliferator-activated receptor gamma (PPARγ) and its transcriptional co-activator PPARγ coactivator-1a (PGC-1a), allowing SIRT1 to participate in the switch between glycolysis and oxidative phosphorylation (83, 84). SIRT1 also impacts metabolism by positively regulating both AMPK and LXRα (85–89). Thus, there are a host of mechanisms by which SIRT1 might regulate AC uptake, many acting downstream of initial ingestion and hence particularly relevant to regulating sustained or delayed AC uptake.

We currently favor two possible, and not mutually-exclusive, roles of SIRT1 in efferocytosis. One relates to our finding that miR-34a expression is down-regulated during enhanced secondary engulfment by AMø. Secondary engulfment has been linked to signaling downstream of AMPK (20) and LXRα (21) in response to lipids and nucleic acids released by digestion of engulfed AC. We suggest that miR-34a and SIRT1 may act as a rheostat controlling activity of AMPK and LXRα in response to AC ingestion. The observed decreased miR-34a expression following efferocytosis in AMø leads through increased

SIRT1 to enhanced AMPK and LXRα signaling, permitting enhanced secondary engulfment in AMø. In contrast, in the virtual absence of miR-34a in PMø, AMPK and LXRα are already highly activated, preventing further augmentation following their initial very efficient efferocytosis. Alternatively, increased SIRT1 as a consequence of miR-34a downregulation might also activate portions of the autophagy machinery, recently shown to be shared with efferocytosis (90). Each of these possibilities merit additional study.

Concluding remarks

We have shown that miR-34a both negatively regulates efferocytosis by resident tissue Mø and is itself down-regulated following AC uptake. Negative regulation of AC uptake by miR-34a appears to depend on the cumulative effect of small changes in the expression of multiple direct and almost certainly additional indirect targets. Because efferocytosis polarizes ingesting Mø uniquely in a manner that is pro-reparative but also detrimental to their host-defense functions, this system may have evolved to fine-tune tissue Mø recognition of AC in specific environments with differing potentials for exposure to microbes.

For the same reasons, strategies to manipulate tissue Mø miR-34a expression hold promise for novel therapeutic approaches in a variety of diseases. Our demonstration that expression of miR-34a in primary human AMø can be reduced using the same specific antagomir validated in murine experiments, and without the need for retroviral transfection, suggests a potential means to test whether improving AMø efferocytic capacity can reduce inflammation in chronic inflammatory lung diseases (52, 91). Investigation of the role of other miRs in the regulation of efferocytosis and its immunological consequents is warranted.

Supplementary Material

Refer to Web version on PubMed Central for supplementary material.

Acknowledgments

NON-STANDARD ABBREVIATIONS

AC   apoptotic cell(s)

AMø   alveolar Mø(s)

AMPK   5' adenosine monophosphate-activated protein kinase

BMDMø	bone marrow-derived Mø
FoxO	forkhead box class O
LCM	lymphocyte culture media
LXRα	Liver X receptor alpha
miR	microRNA(s)
Mø	macrophage(s)
PMø	peritoneal Mø(s)
PPARγ	peroxisome proliferator-activated receptor gamma
SIRT1	Silent Information Regulator T1
wt	wild type

References

1. Nacu N I, Luzina G, Highsmith K, Lockatell V, Pochetuhen K, Cooper ZA, Gillmeister MP, Todd NW, Atamas SP. Macrophages produce TGF-beta-induced (beta-ig-h3) following ingestion of apoptotic cells and regulate MMP14 levels and collagen turnover in fibroblasts. J Immunol. 2008; 180:5036–5044. [PubMed: 18354229]

2. Xiao YQ, Freire-de-Lima CG, Schiemann WP, Bratton DL, Vandivier RW, Henson PM. Transcriptional and translational regulation of TGF-beta production in response to apoptotic cells. J Immunol. 2008; 181:3575–3585. [PubMed: 18714031]

3. Huynh ML V, Fadok A, Henson PM. Phosphatidylserine-dependent ingestion of apoptotic cells promotes TGF-beta1 secretion and the resolution of inflammation. J Clin Invest. 2002; 109:41–50. [PubMed: 11781349]

4. Clancy RM, Buyon JP. Clearance of apoptotic cells: TGF-beta in the balance between inflammation and fibrosis. J Leukoc Biol. 2003; 74:959–960. [PubMed: 12960252]

5. Zhang Y, Kim HJ, Yamamoto S, Kang X, Ma X. Regulation of interleukin-10 gene expression in macrophages engulfing apoptotic cells. J Interferon Cytokine Res. 2010; 30:113–122. [PubMed: 20187777]

6. Chung EY, Liu J, Homma Y, Zhang Y, Brendolan A, Saggese M, Han J, Silverstein R, Selleri L, Ma X. Interleukin-10 expression in macrophages during phagocytosis of apoptotic cells is mediated by homeodomain proteins Pbx1 and Prep-1. Immunity. 2007; 27:952–964. [PubMed: 18093541]

7. Medeiros AI, Serezani CH, Lee SP, Peters-Golden M. Efferocytosis impairs pulmonary macrophage and lung antibacterial function via PGE2/EP2 signaling. J Exp Med. 2009; 206:61–68. [PubMed: 19124657]

8. Hochreiter-Hufford A, Ravichandran KS. Clearing the dead: apoptotic cell sensing, recognition, engulfment, and digestion. Cold Spring Harb Perspect Biol. 2013; 5:a008748. [PubMed: 23284042]

9. Curtis JL, Todt JC, Hu B, Osterholzer JJ, Freeman CM. Tyro3 receptor tyrosine kinases in the heterogeneity of apoptotic cell uptake. Front Biosci. 2009; 14:2631–2646.

10. Seitz HM, Camenisch TD, Lemke G, Earp HS, Matsushima GK. Macrophages and dendritic cells use different Axl/Mertk/Tyro3 receptors in clearance of apoptotic cells. J Immunol. 2007; 178:5635–5642. [PubMed: 17442946]

11. Hu B, Punturieri A, Todt J, Sonstein J, Polak T, Curtis JL. Recognition and phagocytosis of apoptotic T cells by resident murine macrophages requires multiple signal transduction events. J Leukoc Biol. 2002; 71:881–889. [PubMed: 11994514]

12. Todt JC, Hu B, Curtis JL. The receptor tyrosine kinase MerTK activates phospholipase C gamma2 during recognition of apoptotic thymocytes by murine macrophages. J Leukoc Biol. 2004; 75:705–713. [PubMed: 14704368]

13. Kinchen JM, Cabello J, Klingele D, Wong K, Feichtinger R, Schnabel H, Schnabel R, Hengartner MO. Two pathways converge at CED-10 to mediate actin rearrangement and corpse removal in *C. elegans*. Nature. 2005; 434:93–99. [PubMed: 15744306]

14. Park SY, Kang KB, Thapa N, Kim SY, Lee SJ, Kim IS. Requirement of adaptor protein GULP during stabilin-2-mediated cell corpse engulfment. J Biol Chem. 2008; 283:10593–10600. [PubMed: 18230608]

15. Osada Y, Sunatani T, Kim IS, Nakanishi Y, Shiratsuchi A. Signalling pathway involving GULP, MAPK and Rac1 for SR-BI-induced phagocytosis of apoptotic cells. J Biochem. 2009; 145:387–394. [PubMed: 19122200]

16. Lu M, Ravichandran KS. Dock180-ELMO cooperation in Rac activation. Methods Enzymol. 2006; 406:388–402. [PubMed: 16472672]

17. Elliott MR, Ravichandran KS. ELMO1 signaling in apoptotic germ cell clearance and spermatogenesis. Ann N Y Acad Sci. 2010; 1209:30–36. [PubMed: 20958313]

18. Elliott MR, Zheng S, Park D, Woodson RI, Reardon MA, Juncadella IJ, Kinchen JM, Zhang J, Lysiak JJ, Ravichandran KS. Unexpected requirement for ELMO1 in clearance of apoptotic germ cells in vivo. Nature. 2010; 467:333–337. [PubMed: 20844538]

19. Akakura S, Kar B, Singh S, Cho L, Tibrewal N, Sanokawa-Akakura R, Reichman C, Ravichandran KS, Birge RB. C-terminal SH3 domain of CrkII regulates the assembly and function of the DOCK180/ELMO Rac-GEF. J Cell Physiol. 2005; 204:344–351. [PubMed: 15700267]

20. Jiang S, Park DW, Stigler WS, Creighton J, Ravi S, Darley-Usmar V, Zmijewski JW. Mitochondria and AMP-activated protein kinase-dependent mechanism of efferocytosis. J Biol Chem. 2013; 288:26013–26026. [PubMed: 23897815]

21. A-Gonzalez N, Bensinger SJ, Hong C, Beceiro S, Bradley MN, Zelcer N, Deniz J, Ramirez C, Diaz M, Gallardo G, de Galarreta CR, Salazar J, Lopez F, Edwards P, Parks J, Andujar M, Tontonoz P, Castrillo A. Apoptotic cells promote their own clearance and immune tolerance through activation of the nuclear receptor LXR. Immunity. 2009; 31:245–258. [PubMed: 19646905]

22. Anderson C, Zhou S, Sawin E, Horvitz HR, Hurwitz ME. SLI-1 Cbl inhibits the engulfment of apoptotic cells in *C. elegans* through a ligase-independent function. PLoS Genet. 2012; 8:e1003115. [PubMed: 23271977]

23. Hurwitz ME, Vanderzalm PJ, Bloom L, Goldman J, Garriga G, Horvitz HR. Abl kinase inhibits the engulfment of apoptotic cells in *Caenorhabditis elegans*. PLoS Biol. 2009; 7:e99. [PubMed: 19402756]

24. Janssen WJ, McPhillips KA, Dickinson MG, Linderman DJ, Morimoto K, Xiao YQ, Oldham KM, Vandivier RW, Henson PM, Gardai SJ. Surfactant proteins A and D suppress alveolar macrophage phagocytosis via interaction with SIRP alpha. Am J Respir Crit Care Med. 2008; 178:158–167. [PubMed: 18420961]

25. McCubbrey AL, Sonstein J, Ames TM, Freeman CM, Curtis JL. Glucocorticoids relieve collectin-driven suppression of apoptotic cell uptake in murine alveolar macrophages through downregulation of SIRPalpha. J Immunol. 2012; 189:112–119. [PubMed: 22615206]

26. Mondal S, Ghosh-Roy S, Loison F, Li Y, Jia Y, Harris C, Williams DA, Luo HR. PTEN negatively regulates engulfment of apoptotic cells by modulating activation of Rac GTPase. J Immunol. 2011; 187:5783–5794. [PubMed: 22043008]

27. Neukomm LJ, Frei AP, Cabello J, Kinchen JM, Zaidel-Bar R, Ma Z, Haney LB, Hardin J, Ravichandran KS, Moreno S, Hengartner MO. Loss of the RhoGAP SRGP-1 promotes the clearance of dead and injured cells in *Caenorhabditis elegans*. Nat Cell Biol. 2011; 13:79–86. [PubMed: 21170032]

28. Simhadri VR, Andersen JF, Calvo E, Choi SC, Coligan JE, Borrego F. Human CD300a binds to phosphatidylethanolamine and phosphatidylserine, and modulates the phagocytosis of dead cells. Blood. 2012; 119:2799–2809. [PubMed: 22302738]

29. Uderhardt S, Herrmann M, Oskolkova OV, Aschermann S, Bicker W, Ipseiz N, Sarter K, Frey B, Rothe T, Voll R, Nimmerjahn F, Bochkov VN, Schett G, Kronke G. 12/15-lipoxygenase orchestrates the clearance of apoptotic cells and maintains immunologic tolerance. Immunity. 2012; 36:834–846. [PubMed: 22503541]

30. Taganov KD, Boldin MP, Baltimore D. MicroRNAs and immunity: tiny players in a big field. Immunity. 2007; 26:133–137. [PubMed: 17307699]

31. Kozomara A, Griffiths-Jones S. miRBase: annotating high confidence microRNAs using deep sequencing data. Nucleic Acids Res. 2014; 42:D68–73. [PubMed: 24275495]

32. Friedman RC, Farh KK, Burge CB, Bartel DP. Most mammalian mRNAs are conserved targets of microRNAs. Genome Res. 2009; 19:92–105. [PubMed: 18955434]

33. Farh KK, Grimson A, Jan C, Lewis BP, Johnston WK, Lim LP, Burge CB, Bartel DP. The widespread impact of mammalian microRNAs on mRNA repression and evolution. Science. 2005; 310:1817–1821. [PubMed: 16308420]

34. El Gazzar M, McCall CE. MicroRNAs distinguish translational from transcriptional silencing during endotoxin tolerance. J Biol Chem. 2010; 285:20940–20951. [PubMed: 20435889]

35. Boon RA, Iekushi K, Lechner S, Seeger T, Fischer A, Heydt S, Kaluza D, Treguer K, Carmona G, Bonauer A, Horrevoets AJ, Didier N, Girmatsion Z, Biliczki P, Ehrlich JR, Katus HA, Muller OJ, Potente M, Zeiher AM, Hermeking H, Dimmeler S. MicroRNA-34a regulates cardiac ageing and function. Nature. 2013; 495:107–110. [PubMed: 23426265]

36. Das A, Ganesh K, Khanna S, Sen CK, Roy S. Engulfment of apoptotic cells by macrophages: a role of microRNA-21 in the resolution of wound inflammation. J Immunol. 2014; 192:1120–1129. [PubMed: 24391209]

37. Concepcion CP, Han YC, Mu P, Bonetti C, Yao E, D'Andrea A, Vidigal JA, Maughan WP, Ogrodowski P, Ventura A. Intact p53-dependent responses in miR-34-deficient mice. PLoS Genet. 2012; 8:e1002797. [PubMed: 22844244]

38. Swanson JA. Phorbol esters stimulate macropinocytosis and solute flow through macrophages. J Cell Sci. 1989; 94(Pt 1):135–142. [PubMed: 2613767]

39. Esen N, Kielian T. Recognition of *Staphylococcus aureus*-derived peptidoglycan (PGN) but not intact bacteria is mediated by CD14 in microglia. J Neuroimmunol. 2005; 170:93–104. [PubMed: 16229899]

40. Esen N, Blakely PK, Rainey-Barger EK, Irani DN. Complexity of the microglial activation pathways that drive innate host responses during lethal alphavirus encephalitis in mice. ASN Neuro. 2012; 4:207–221. [PubMed: 22471445]

41. Todt JC, Freeman CM, Brown JP, Sonstein J, Ames TM, McCubbrey AL, Martinez FJ, Chensue SW, Beck JM, Curtis JL. Smoking decreases the response of human lung macrophages to double-stranded RNA by reducing TLR3 expression. Respir Res. 2013; 14:33. [PubMed: 23497334]

42. Licht R, Jacobs CW, Tax WJ, Berden JH. An assay for the quantitative measurement of in vitro phagocytosis of early apoptotic thymocytes by murine resident peritoneal macrophages. J Immunol Methods. 1999; 223:237–248. [PubMed: 10089102]

43. Culpitt SV, Rogers DF, Fenwick PS, Shah P, De Matos C, Russell RE, Barnes PJ, Donnelly LE. Inhibition by red wine extract, resveratrol, of cytokine release by alveolar macrophages in COPD. Thorax. 2003; 58:942–946. [PubMed: 14586044]

44. Knobloch J, Hag H, Jungck D, Urban K, Koch A. Resveratrol impairs the release of steroid-resistant cytokines from bacterial endotoxin-exposed alveolar macrophages in chronic obstructive pulmonary disease. Basic Clin Pharmacol Toxicol. 2011; 109:138–143. [PubMed: 21447053]

45. Yang SR, Wright J, Bauter M, Seweryniak K, Kode A, Rahman I. Sirtuin regulates cigarette smoke-induced proinflammatory mediator release via RelA/p65 NF-kappaB in macrophages in vitro and in rat lungs in vivo: implications for chronic inflammation and aging. Am J Physiol Lung Cell Mol Physiol. 2007; 292:L567–576. [PubMed: 17041012]

46. Hwang JW, Chung S, Sundar IK, Yao H, Arunachalam G, McBurney MW, Rahman I. Cigarette smoke-induced autophagy is regulated by SIRT1-PARP-1-dependent mechanism: implication in pathogenesis of COPD. Arch Biochem Biophys. 2010; 500:203–209. [PubMed: 20493163]

47. Peck B, Chen CY, Ho KK, Di Fruscia P, Myatt SS, Coombes RC, Fuchter MJ, Hsiao CD, Lam EW. SIRT inhibitors induce cell death and p53 acetylation through targeting both SIRT1 and SIRT2. Mol Cancer Ther. 2010; 9:844–855. [PubMed: 20371709]

48. Jia Y, Zheng Z, Wang Y, Zhou Q, Cai W, Jia W, Yang L, Dong M, Zhu X, Su L, Hu D. SIRT1 is a regulator in high glucose-induced inflammatory response in RAW264.7 cells. PLoS One. 2015; 10:e0120849. [PubMed: 25793995]

49. Park D, Han CZ, Elliott MR, Kinchen JM, Trampont PC, Das S, Collins S, Lysiak JJ, Hoehn KL, Ravichandran KS. Continued clearance of apoptotic cells critically depends on the phagocyte Ucp2 protein. Nature. 2011; 477:220–224. [PubMed: 21857682]

50. Park D, Tosello-Trampont AC, Elliott MR, Lu M, Haney LB, Ma Z, Klibanov AL, Mandell JW, Ravichandran KS. BAI1 is an engulfment receptor for apoptotic cells upstream of the ELMO/Dock180/Rac module. Nature. 2007; 450:430–434. [PubMed: 17960134]

51. Canbay A, Taimr P, Torok N, Higuchi H, Friedman S, Gores GJ. Apoptotic body engulfment by a human stellate cell line is profibrogenic. Lab Invest. 2003; 83:655–663. [PubMed: 12746475]

52. McCubbrey AL, Curtis JL. Efferocytosis and lung disease. Chest. 2013; 143:1750–1757. [PubMed: 23732585]

53. Hodge S, Hodge G, Ahern J, Jersmann H, Holmes M, Reynolds PN. Smoking alters alveolar macrophage recognition and phagocytic ability: implications in chronic obstructive pulmonary disease. Am J Respir Cell Mol Biol. 2007; 37:748–755. [PubMed: 17630319]

54. Richens TR, Linderman DJ, Horstmann SA, Lambert C, Xiao YQ, Keith RL, Boe DM, Morimoto K, Bowler RP, Day BJ, Janssen WJ, Henson PM, Vandivier RW. Cigarette smoke impairs clearance of apoptotic cells through oxidant-dependent activation of RhoA. Am J Respir Crit Care Med. 2009; 179:1011–1021. [PubMed: 19264974]

55. Mackiewicz M, Huppi K, Pitt JJ, Dorsey TH, Ambs S, Caplen NJ. Identification of the receptor tyrosine kinase AXL in breast cancer as a target for the human miR-34a microRNA. Breast Cancer Res Treat. 2011; 130:663–679. [PubMed: 21814748]

56. Lemke G, Burstyn-Cohen T. TAM receptors and the clearance of apoptotic cells. Ann N Y Acad Sci. 2010; 1209:23–29. [PubMed: 20958312]

57. Yamakuchi M, Ferlito M, Lowenstein CJ. miR-34a repression of SIRT1 regulates apoptosis. Proc Natl Acad Sci U S A. 2008; 105:13421–13426. [PubMed: 18755897]

58. Coussens M, Maresh JG, Yanagimachi R, Maeda G, Allsopp R. Sirt1 deficiency attenuates spermatogenesis and germ cell function. PLoS One. 2008; 3:e1571. [PubMed: 18270565]

59. Sequeira J, Boily G, Bazinet S, Saliba S, He X, Jardine K, Kennedy C, Staines W, Rousseaux C, Mueller R, McBurney MW. sirt1-null mice develop an autoimmune-like condition. Exp Cell Res. 2008; 314:3069–3074. [PubMed: 18687325]

60. Martin CJ, Peters KN, Behar SM. Macrophages clean up: efferocytosis and microbial control. Curr Opin Microbiol. 2014; 17:17–23. [PubMed: 24581688]

61. Juncadella IJ, Kadl A, Sharma AK, Shim YM, Hochreiter-Hufford A, Borish L, Ravichandran KS. Apoptotic cell clearance by bronchial epithelial cells critically influences airway inflammation. Nature. 2013; 493:547–551. [PubMed: 23235830]

62. Grandbarbe L, Michelucci A, Heurtaux T, Hemmer K, Morga E, Heuschling P. Notch signaling modulates the activation of microglial cells. Glia. 2007; 55:1519–1530. [PubMed: 17705199]

63. Monsalve E, Perez MA, Rubio A, Ruiz-Hidalgo MJ, Baladron V, Garcia-Ramirez JJ, Gomez JC, Laborda J, Diaz-Guerra MJ. Notch-1 up-regulation and signaling following macrophage activation modulates gene expression patterns known to affect antigen-presenting capacity and cytotoxic activity. J Immunol. 2006; 176:5362–5373. [PubMed: 16622004]

64. Hashimi ST, Fulcher JA, Chang MH, Gov L, Wang S, Lee B. MicroRNA profiling identifies miR-34a and miR-21 and their target genes JAG1 and WNT1 in the coordinate regulation of dendritic cell differentiation. Blood. 2009; 114:404–414. [PubMed: 19398721]

65. Li Y, Guessous F, Zhang Y, Dipierro C, Kefas B, Johnson E, Marcinkiewicz L, Jiang J, Yang Y, Schmittgen TD, Lopes B, Schiff D, Purow B, Abounader R. MicroRNA-34a inhibits glioblastoma growth by targeting multiple oncogenes. Cancer Res. 2009; 69:7569–7576. [PubMed: 19773441]

66. Kaller M, Liffers ST, Oeljeklaus S, Kuhlmann K, Roh S, Hoffmann R, Warscheid B, Hermeking H. Genome-wide characterization of miR-34a induced changes in protein and mRNA expression by a combined pulsed SILAC and microarray analysis. Mol Cell Proteomics. 2011; 10:M111 010462. [PubMed: 21566225]

67. Neukomm LJ, Nicot AS, Kinchen JM, Almendinger J, Pinto SM, Zeng S, Doukoumetzidis K, Tronchere H, Payrastre B, Laporte JF, Hengartner MO. The phosphoinositide phosphatase MTM-1 regulates apoptotic cell corpse clearance through CED-5-CED-12 in *C. elegans*. Development. 2011; 138:2003–2014. [PubMed: 21490059]

68. Morimoto K, Janssen WJ, Fessler MB, McPhillips KA, Borges VM, Bowler RP, Xiao YQ, Kench JA, Henson PM, Vandivier RW. Lovastatin enhances clearance of apoptotic cells (efferocytosis) with implications for chronic obstructive pulmonary disease. J Immunol. 2006; 176:7657–7665. [PubMed: 16751413]

69. Hodge S, Hodge G, Brozyna S, Jersmann H, Holmes M, Reynolds PN. Azithromycin increases phagocytosis of apoptotic bronchial epithelial cells by alveolar macrophages. Eur Respir J. 2006; 28:486–495. [PubMed: 16737992]

70. Hu B, Jennings JH, Sonstein J, Floros J, Todt JC, Polak T, Curtis JL. Resident murine alveolar and peritoneal macrophages differ in adhesion of apoptotic thymocytes. Am J Respir Cell Mol Biol. 2004; 30:687–693. [PubMed: 14527926]

71. Monick MM, Carter AB, Gudmundsson G, Geist LJ, Hunninghake GW. Changes in PKC isoforms in human alveolar macrophages compared with blood monocytes. Am J Physiol. 1998; 275:L389–397. [PubMed: 9700101]

72. Todt JC, Hu B, Punturieri A, Sonstein J, Polak T, Curtis JL. Activation of protein kinase C beta II by the stereo-specific phosphatidylserine receptor is required for phagocytosis of apoptotic thymocytes by resident murine tissue macrophages. J Biol Chem. 2002; 277:35906–35914. [PubMed: 12114511]

73. Hermeking H. The miR-34 family in cancer and apoptosis. Cell Death Differ. 2010; 17:193–199. [PubMed: 19461653]

74. Yamakuchi M, Lowenstein CJ. MiR-34, SIRT1 and p53: the feedback loop. Cell Cycle. 2009; 8:712–715. [PubMed: 19221490]

75. Bader AG. miR-34 - a microRNA replacement therapy is headed to the clinic. Front Genet. 2012; 3:120. [PubMed: 22783274]

76. Tazawa H, Tsuchiya N, Izumiya M, Nakagama H. Tumor-suppressive miR-34a induces senescence-like growth arrest through modulation of the E2F pathway in human colon cancer cells. Proc Natl Acad Sci U S A. 2007; 104:15472–15477. [PubMed: 17875987]

77. Welch C, Chen Y, Stallings RL. MicroRNA-34a functions as a potential tumor suppressor by inducing apoptosis in neuroblastoma cells. Oncogene. 2007; 26:5017–5022. [PubMed: 17297439]

78. Wiggins JF, Ruffino L, Kelnar K, Omotola M, Patrawala L, Brown D, Bader AG. Development of a lung cancer therapeutic based on the tumor suppressor microRNA-34. Cancer Res. 2010; 70:5923–5930. [PubMed: 20570894]

79. Kroemer G, Galluzzi L, Kepp O, Zitvogel L. Immunogenic cell death in cancer therapy. Annu Rev Immunol. 2013; 31:51–72. [PubMed: 23157435]

80. Liu B, Zhang B, Guo R, Li S, Xu Y. Enhancement in efferocytosis of oxidized low-density lipoprotein-induced apoptotic RAW264.7 cells through Sirt1-mediated autophagy. Int J Mol Med. 2014; 33:523–533. [PubMed: 24378473]

81. Chen F, Hu SJ. Effect of microRNA-34a in cell cycle, differentiation, and apoptosis: a review. J Biochem Mol Toxicol. 2012; 26:79–86. [PubMed: 22162084]

82. Ng F, Tang BL. Sirtuins' modulation of autophagy. J Cell Physiol. 2013; 228:2262–2270. [PubMed: 23696314]

83. Rodgers JT, Lerin C, Haas W, Gygi SP, Spiegelman BM, Puigserver P. Nutrient control of glucose homeostasis through a complex of PGC-1alpha and SIRT1. Nature. 2005; 434:113–118. [PubMed: 15744310]

84. Liu TF V, Vachharajani T, Yoza BK, McCall CE. NAD+-dependent sirtuin 1 and 6 proteins coordinate a switch from glucose to fatty acid oxidation during the acute inflammatory response. J Biol Chem. 2012; 287:25758–25769. [PubMed: 22700961]

85. Gu XS, Wang ZB, Ye Z, Lei JP, Li L, Su DF, Zheng X. Resveratrol, an activator of SIRT1, upregulates AMPK and improves cardiac function in heart failure. Genet Mol Res. 2014; 13:323–335. [PubMed: 24535859]

86. Li X, Zhang S, Blander G, Tse JG, Krieger M, Guarente L. SIRT1 deacetylates and positively regulates the nuclear receptor LXR. Mol Cell. 2007; 28:91–106. [PubMed: 17936707]

87. Price NL, Gomes AP, Ling AJ, Duarte FV, Martin-Montalvo A, North BJ, Agarwal B, Ye L, Ramadori G, Teodoro JS, Hubbard BP, Varela AT, Davis JG, Varamini B, Hafner A, Moaddel R, Rolo AP, Coppari R, Palmeira CM, de Cabo R, Baur JA, Sinclair DA. SIRT1 is required for

AMPK activation and the beneficial effects of resveratrol on mitochondrial function. Cell Metab. 2012; 15:675–690. [PubMed: 22560220]

88. Hou X, Xu S, Maitland-Toolan KA, Sato K, Jiang B, Ido Y, Lan F, Walsh K, Wierzbicki M, Verbeuren TJ, Cohen RA, Zang M. SIRT1 regulates hepatocyte lipid metabolism through activating AMP-activated protein kinase. J Biol Chem. 2008; 283:20015–20026. [PubMed: 18482975]

89. Chen S, Xiao X, Feng X, Li W, Zhou N, Zheng L, Sun Y, Zhang Z, Zhu W. Resveratrol induces Sirt1-dependent apoptosis in 3T3-L1 preadipocytes by activating AMPK and suppressing AKT activity and survivin expression. J Nutr Biochem. 2012; 23:1100–1112. [PubMed: 22137261]

90. Martinez J, Almendinger J, Oberst A, Ness R, Dillon CP, Fitzgerald P, Hengartner MO, Green DR. Microtubule-associated protein 1 light chain 3 alpha (LC3)-associated phagocytosis is required for the efficient clearance of dead cells. Proc Natl Acad Sci U S A. 2011; 108:17396–17401. [PubMed: 21969579]

91. Henson PM, Cosgrove GP, Vandivier RW. State of the art. Apoptosis and cell homeostasis in chronic obstructive pulmonary disease. Proc Am Thorac Soc. 2006; 3:512–516. [PubMed: 16921132]
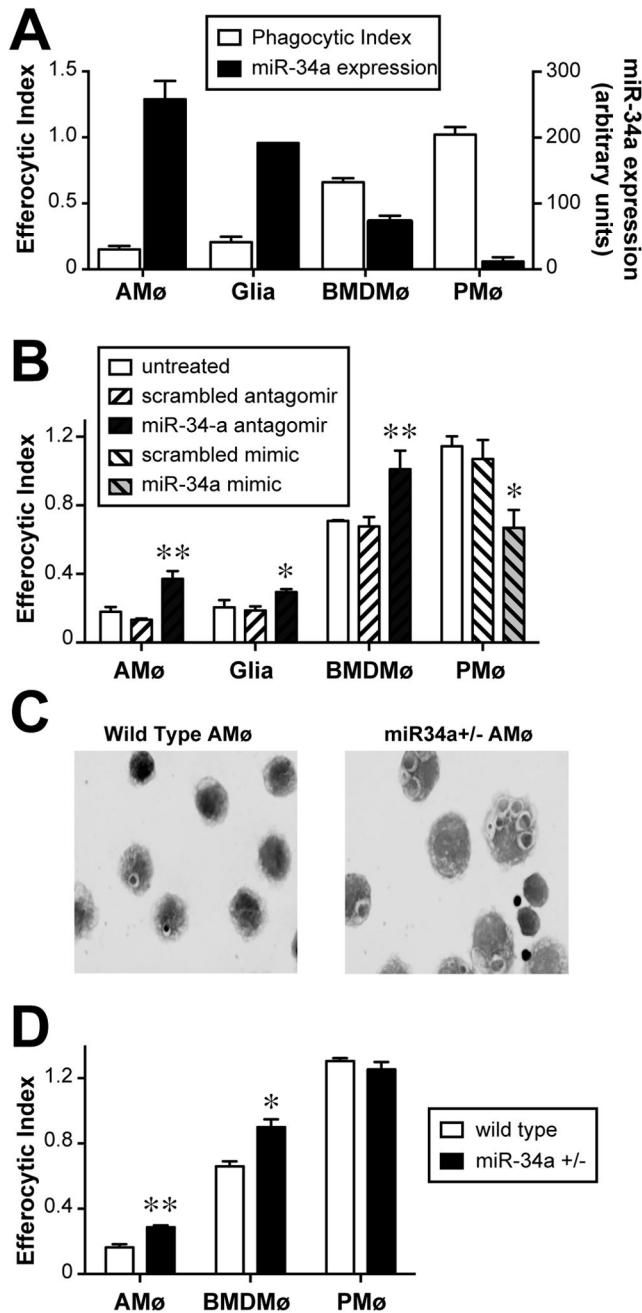
Figure 1. miR-34a negatively regulates efferocytosis

A. AMø, glia, BMDMø and PMø were either incubated with AC in chamber slides for 1.5 h, then stained using H&E and assayed for efferocytosis (left-hand axis), or were assayed by quantitative real-time RT-PCR for expression of miR-34a relative to sno-142 (right-hand axis). Note inverse relationship between phagocytic index and miR-34a expression. Data are mean ± SEM of at least three replicates of each cell type from two independent experiments.

B. Using RNAiMAX Lipofectamine, AMø, glia, BMDMø were transfected with control or miR-34a-specific antagomirs and PMø were transfected with control or miR-34a-specific mimics. AC engulfment was assessed by microscopy after 1.5 h. Data are mean ± SEM of at

least three replicates of each cell type from two independent experiments; *, p<0.05; **, p<0.01 by one-way ANOVA with Bonferroni post-hoc testing. C, D. miR-34a flox/flox mice were crossed with LysM cre mice resulting in miR-34a flox/−, LysM cre offspring (miR-34a+/−) with miR-34a haplosufficient myeloid cells. Resident AMø, PMø and BMDMø harvested form wt mice and miR-34a +/− mice were exposed to AC in chamber slides for 1.5 h, then washed, stained with H&E and counted. C. Representative photos of in vitro AC engulfment by AMø of wt mice (left) and AMø of miR-34a +/− mice (right) (1000x final magnification). D. Phagocytic index, as mean ± SEM from n=4–7 mice from 2–4 independent experiments per cell type; *, p<0.05; **, p<0.01 by Student t test.
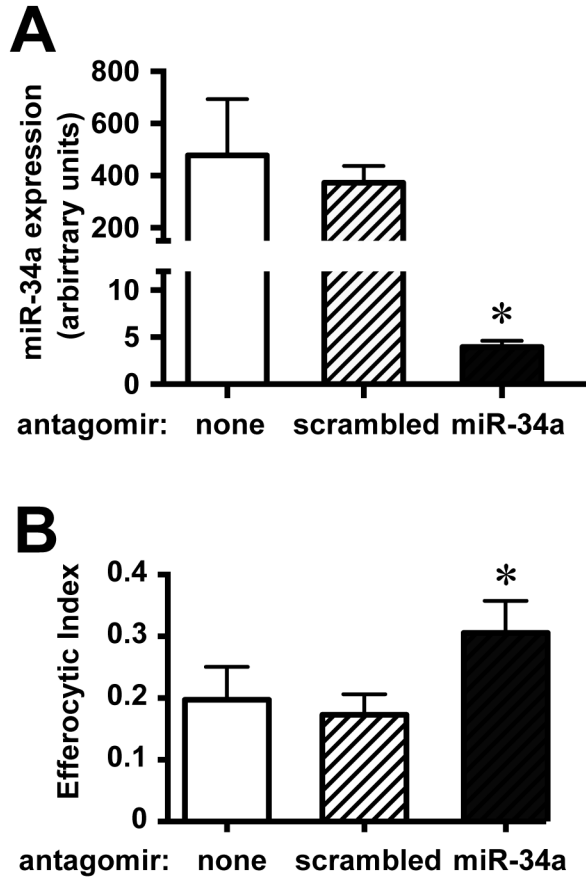
A

B

Figure 2. miR-34a negatively regulates efferocytosis by human AMø

AMø were harvested by bronchoalveolar lavage of healthy human never-smoker volunteers and transfected in vitro using control (scrambled) or miR-34a-specific antagomirs using RNAiMAX lipofectamine. Following transfection, AMø were either (A) processed to isolate total RNA, which was assayed by quantitative real-time PCR; or (B) exposed to AC for 90 min and then assayed for efferocytosis in chamber slides, which were H&E-stained and counted by microscopy. Data are mean ± SEM of individual subjects in independent experiments, A, *n*=3; B, *n*=4; *, p<0.05 by one-way ANOVA with Bonferroni post-hoc testing.
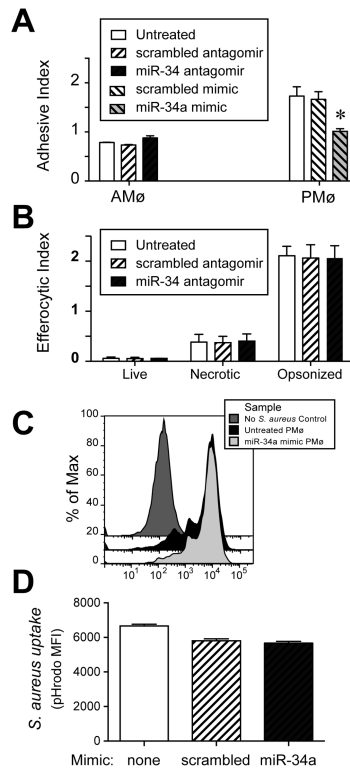
Figure 3. miR-34a negatively regulates binding to AC but not uptake of other targets

A–D. Using RNAiMAX Lipofectamine and chamber slides, murine AMø were transfected with control or miR-34a-specific antagomirs (24 h incubation) and murine PMø were transfected with control or miR-34a-specific mimics (48 h incubation). A. AC adhesion by transfected AMø and PMø was assessed by histology after 15 min. Data are mean ± SEM of three independent experiments. B. Phagocytosis by transfected AMø was assessed by microscopy after 1.5 h exposure of AMø to live thymocytes, necrotic thymocytes, or opsonized SRBC. Data are mean ± SEM of at least three independent experiments per target cell type. C, D. Phagocytosis by transfected PMø of pHrodo-labeled, Ig-opsonized-*S. aureus* following 1 h exposure, then release and analysis by flow cytometry. C. Representative histogram showing pHrodo staining. D. Uptake as measured by pHrodo MFI; data are mean ± SEM from n=3 mice assayed individually in each of two independent experiments, p<0.05 by one-way ANOVA with Bonferroni post-hoc testing.
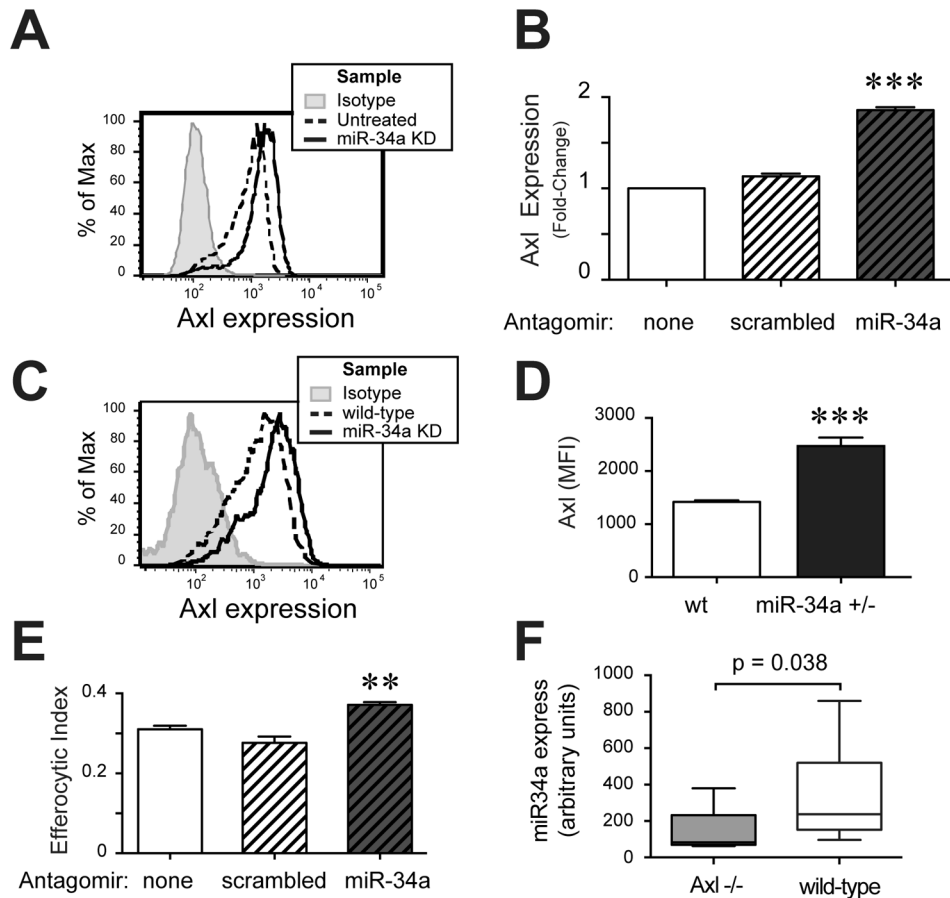
Figure 4. miR-34a regulates Mø expression of Axl, but altered Axl expression is not required for regulation of efferocytosis

A, B. AMø from wt mice were transfected with control scrambled antagomirs (scrambled) or miR-34a-specific antagomirs (miR-34a KD) using RNAiMAX lipofectamine. Following knockdown, AMø were stained for surface expression of Axl and assayed by flow cytometry, gating AMø as CD45+ CD11c+ cells. A. Representative histograms; isotype, grey; untreated, dashed line; miR-34a+/− KD, solid line; scrambled antagomir-treated omitted for clarity. B. Data are expressed as fold change in MFI, relative to untreated AMø and are presented as mean ± SEM of as least four replicates in each of three independent experiments; ***, $p<0.001$ significantly different from both other groups, one-way ANOVA with Tukey post-hoc testing. C, D. BMDMø harvested from wt mice and miR-34a+/− mice were surface stained for Axl and analyzed by flow cytometry, gating on CD45+ cells. C. Representative histogram of Axl staining (isotype, grey; wt BMDMø, dashed line; miR-34a +/− BMDMø, solid line). D. Axl MFI; data are mean ± SEM of eight mice of each genotype in three independent experiments; ***, $p<0.001$, Mann-Whitney U test. E. BMDMø from Axl−/− mice were transfected with scrambled or miR-34a-specific antagomirs using RNAiMAX Lipofectamine, then exposed to AC for 90 min and assayed for efferocytosis by microscopy; data are mean ± SEM of duplicate or triplicate samples from three separate BMDMø cultures; **, $p<0.01$ by one-way ANOVA with Tukey post-hoc testing. F. miR-34a mRNA expression of BMDMø from Axl −/− mice (grary) or wild-type mice

(white) was assayed by quantitative real-time PCR, relative to RNU6B; data are median, IQR and 95, 5% CI of eight independent bone marrow cultures assayed in four independent expreiments; Mann-Whitney U test.
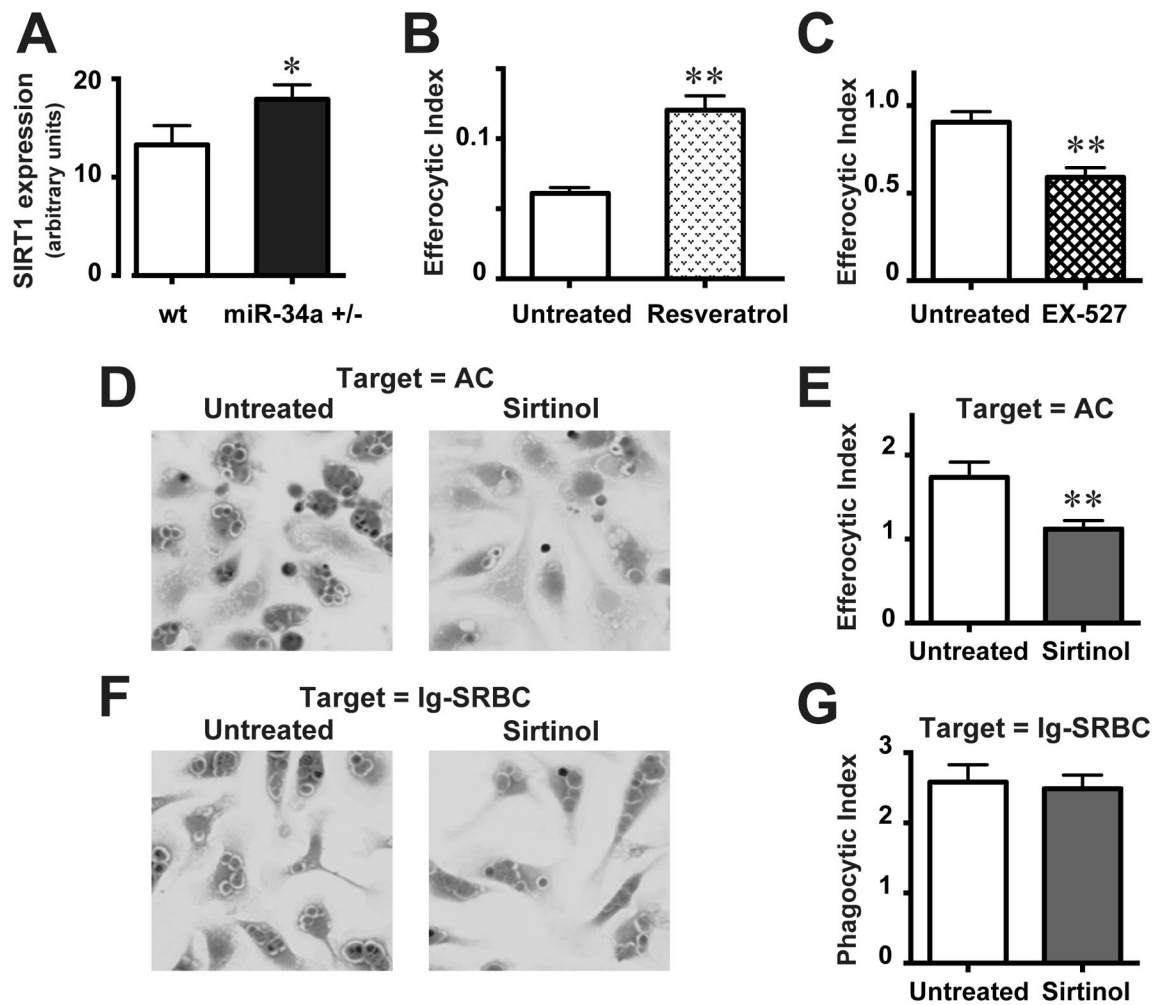
Figure 5. miR-34a negatively regulates Mø SIRT1 expression and SIRT1 enhances efferocytosis
A. Total RNA was harvested from AMø of wt mice and miR-34a+/− mice and SIRT1 mRNA expression was assessed by quantitative real-time RT-PCR, relative to GAPDH. B. Resident AMø from wt mice were treated in chamber-slides with the SIRT1-agonist resveratrol (10 μM for 24 h), exposed to AC and then efferocytosis was measured by microscopy. C–E. Resident PMø from wt mice were treated in chamber-slides with the SIRT1-antagonists (C) EX-527 (10 μM for 24 h) or (D, E) sirtinol (10 μM for 24 h), exposed to AC for 90 min, washed using a systematic protocol, stained using H&E and then efferocytosis was measured by microscopy. (F, G) Resident PMø from wt mice were treated in chamber-slides with the SIRT1-antagonist sirtinol (10 μM for 24 h), exposed to Ig-opsonized SRBC for 60 min, washed using a systematic protocol, stained using H&E and then FcγR-mediated uptake was measured by microscopy. Representative photomicrographs (D, F) are H&E-stained at 1000 X magnification. Data in all graphs are mean ± SEM from at least four replicates from two or more independent experiments. *, $p < 0.05$; **, $p < 0.01$ by Student t test.
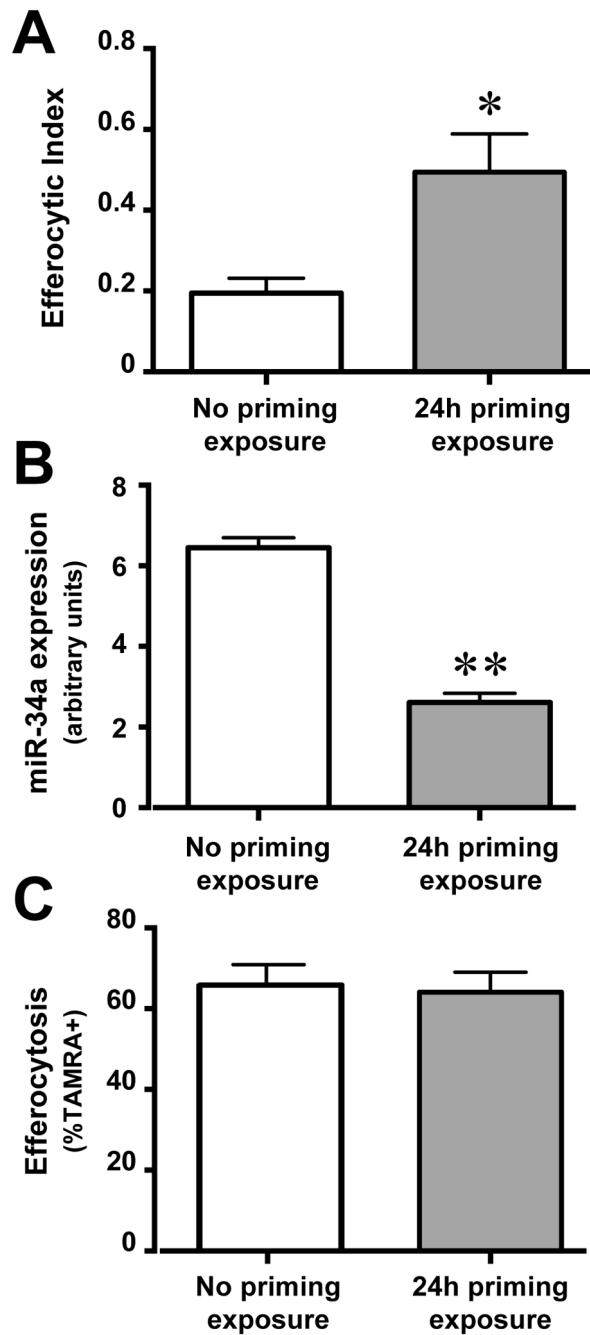
Figure 6. Efferocytosis down-regulates miR-34a, creating a positive-feedback loop for secondary engulfment

A. Resident AMø from wt mice were exposed to AC f for 2 h, then AC were removed by vigorous washing and AMø were incubated in LCM for a further 22 h before a second aliquot of AC were added and efferocytosis was assayed after 90 min using a microscopy assay of H&E stained slides. B. Resident AMø from wt mice were exposed to AC or LCM for 24 h, washed to remove unbound AC and then total RNA was harvested; expression of miR-34a, relative to sno-142, was assessed using quantitative real-time RT-PCR. C. Resident PMø from wt mice were exposed to AC twice, exactly as in panel A, except that in

the second exposure, AC were TAMRA-labeled and efferocytosis was assayed after 60 min using flow cytometry. C. Data in all graphs are mean ± SEM from at least four replicates from two or more independent experiments. *, $p < 0.05$; **, $p < 0.01$ by Student t test.

Table I

Characteristics of human subjects

Age	Sex	FEV1 % predicted	FEV1/FVC ratio	Smoking status	Smoking history (pack-years)
36	Female	93	0.90	Never	0
57	Female	110	0.71	Never	0
25	Female	97	0.84	Never	0
27	Female	105	0.91	Never	0
50	Female	103	0.84	Current	10.3
56	Female	86	0.86	Current	7.7